JCI The Journal of Clinical Investigation

The α_{1D}-adrenergic receptor directly regulates arterial blood pressure via vasoconstriction

Akito Tanoue, … , Satoshi Takeo, Gozoh Tsujimoto

J Clin Invest. 2002;109(6):765-775. https://doi.org/10.1172/JCI14001.

Article Genetics

To investigate the physiological role of the α_{1D}-adrenergic receptor (α_{1D}-AR) subtype, we created mice lacking the α_{1D}-AR ($\alpha_{1D}^{-/-}$) by gene targeting and characterized their cardiovascular function. In $\alpha_{1D}^{-/-}$ mice, the RT-PCR did not detect any transcript of the α_{1D}-AR in any tissue examined, and there was no apparent upregulation of other α_1-AR subtypes. Radioligand binding studies showed that α_1-AR binding capacity in the aorta was lost, while that in the heart was unaltered in $\alpha_{1D}^{-/-}$ mice. Non-anesthetized $\alpha_{1D}^{-/-}$ mice maintained significantly lower basal systolic and mean arterial blood pressure conditions, relative to wild-type mice, and they showed no significant change in heart rate or in cardiac function, as assessed by echocardiogram. Besides hypotension, the pressor responses to phenylephrine and norepinephrine were decreased by 30–40% in $\alpha_{1D}^{-/-}$ mice. Furthermore, the contractile response of the aorta and the pressor response of isolated perfused mesenteric arterial beds to α_1-AR stimulation were markedly reduced in $\alpha_{1D}^{-/-}$ mice. We conclude that the α_{1D}-AR participates directly in sympathetic regulation of systemic blood pressure by vasoconstriction.

The α_{1D}-adrenergic receptor directly regulates arterial blood pressure via vasoconstriction

Akito Tanoue,[1] Yoshihisa Nasa,[2] Takaaki Koshimizu,[1] Hitomi Shinoura,[1] Sayuri Oshikawa,[1] Takayuki Kawai,[2] Sachie Sunada,[2] Satoshi Takeo,[2] and Gozoh Tsujimoto[1]

[1]Department of Molecular, Cell Pharmacology, National Children's Medical Research Center, Tokyo, Japan
[2]Department of Pharmacology, Tokyo University of Pharmacy and Life Science, Tokyo, Japan

Address correspondence to: Gozoh Tsujimoto, Department of Molecular, Cell Pharmacology, National Children's Medical Research Center, 3-35-31, Taishido, Setagaya-ku, Tokyo, 154-8509, Japan. Phone: 81-3-3419-2476; Fax: 81-3-3419-1252; E-mail: gtsujimoto@nch.go.jp.

Received for publication September 24, 2001, and accepted in revised form February 4, 2002.

To investigate the physiological role of the α_{1D}-adrenergic receptor (α_{1D}-AR) subtype, we created mice lacking the α_{1D}-AR ($\alpha_{1D}^{-/-}$) by gene targeting and characterized their cardiovascular function. In $\alpha_{1D}^{-/-}$ mice, the RT-PCR did not detect any transcript of the α_{1D}-AR in any tissue examined, and there was no apparent upregulation of other α_1-AR subtypes. Radioligand binding studies showed that α_1-AR binding capacity in the aorta was lost, while that in the heart was unaltered in $\alpha_{1D}^{-/-}$ mice. Non-anesthetized $\alpha_{1D}^{-/-}$ mice maintained significantly lower basal systolic and mean arterial blood pressure conditions, relative to wild-type mice, and they showed no significant change in heart rate or in cardiac function, as assessed by echocardiogram. Besides hypotension, the pressor responses to phenylephrine and norepinephrine were decreased by 30–40% in $\alpha_{1D}^{-/-}$ mice. Furthermore, the contractile response of the aorta and the pressor response of isolated perfused mesenteric arterial beds to α_1-AR stimulation were markedly reduced in $\alpha_{1D}^{-/-}$ mice. We conclude that the α_{1D}-AR participates directly in sympathetic regulation of systemic blood pressure by vasoconstriction.

J. Clin. Invest. **109**:765–775 (2002). DOI:10.1172/JCI200214001.

Introduction

The sympathetic nervous system plays an important role in regulating the tone of the peripheral circulation and hence in the control of blood pressure. Catecholamines cause vascular smooth muscle contraction by activating α_1-adrenergic receptors (α_1-ARs) (1). Recent extensive efforts have been made to classify the three known α_1-AR subtypes (α_{1A}, α_{1B}, and α_{1D}) by molecular cloning (2–7) and pharmacological analyses (8–11); however, the contribution of each α_1-AR subtype to catecholamine-induced physiological responses still has not been well characterized (12, 13). Studies aimed at assessing functional role(s) mediated by distinct α_1-AR subtypes have been hampered, in part because the available subtype-selective drugs are only moderately selective and may interact with other adrenergic and nonadrenergic receptors and because native tissues can express all three subtypes. Thus, the functional implications of α_1-AR heterogeneity and their physiological relevance remain largely unknown.

Gene disruption (knockout) experiments have proved to be useful in defining the function of a target molecule in vivo. Gene targeting of each receptor subtype ought to be useful in determining their functional role(s). The power to reveal novel functions and mechanisms of action can be greatly enhanced when pharmacological tools are used in conjunction with these genetic techniques (14, 15). Among the three α_1-AR subtypes, this technique has been used to disrupt expression of the α_{1B}-AR subtype (16). α_{1B}-AR knockout mice were shown to be normotensive, but displayed a moderate decrease in pressor responses to α_1-AR stimulation (16), providing evidence that the α_{1B}-AR participates in the regulation of vasoconstriction and hence blood pressure. However, pharmacological studies with the "α_{1D}-AR–selective" antagonist BMY7378 suggest that the α_{1D}-AR plays a predominant role in the vascular contractions induced by α_1-AR agonists in the rat (17). Also, by examining transgenic mice overexpressing the α_{1B}-AR Zuscik et al. (18) very recently have reported that the α_{1B}-AR is not directly involved in blood pressure–related vasoconstriction. Hence, the functional role of the α_{1D}-AR in the control of vascular tone and blood pressure needs to be clarified.

In this study, we describe the gene targeting of the mouse α_{1D}-AR and the initial functional characterization of knockout mice lacking this receptor subtype. The clinical efficacy of α_1-AR antagonists as antihypertensive drugs reflects the important physiological role of α_1-ARs in vascular function and in the maintenance of arterial blood pressure. We therefore focused on functional characterization of the α_{1D}-AR knockout model in terms of cardiovascular functions. Our study shows that the α_{1D}-AR is a mediator of the vasoconstrictive and pressor responses to catecholamines.

Methods

Gene targeting. The murine α_{1D}-AR gene consists of two exons and one intron, spanning more than 10 kb (19). Restriction fragments of 3 kb (*Hind*III/*Sac*II) and 5 kb (*Sac*I/*Sal*I) were subcloned from the mouse α_{1D}-AR genomic clone (Figure 1) into pBlueScript. These two fragments were inserted into a plasmid with a 1.6-kb cassette containing the neomycin resistance gene (Neo), under the control of the phosphoglycerate kinase promoter, as described (20). As a result, the 0.3-kb *Sac*I-*Sac*II region, including the first AUG codon (–131 to +181, relative to AUG initiation codon), in the first exon of the α_{1D}-AR gene was replaced with the Neo cassette. The diphtheria toxin A fragment gene was used as a negative selection marker (21). The 1.8-kb diphtheria toxin cassette (DT) was inserted into the plasmid to obtain the targeting vector NeoDT (Figure 1). After its linearization with *Not*I, the targeting vector contained two regions of homology with the α_{1D}-AR gene: 3 kb of the 5′ untranslated sequences flanking the first exon and a 5-kb fragment containing the first exon and intron. The linearized targeting vector was electroporated into 129Sv embryonic stem (ES) cells, which were then subjected to selection with G418. Southern blot analysis was performed on 288 neomycin-resistant ES cell clones. Genomic DNA was digested with *Eco*RI, electrophoresed on a 0.8% agarose gel, transferred to a membrane, and hybridized with the 5′ probe, derived from the α_{1D}-AR locus (Figure 1). Digestion of genomic DNA with *Eco*RI generated 12-kb and 4-kb restriction fragments for the wild-type and disrupted alleles, respectively. Seven clones positive for the 5′ probe were expanded and subjected to further Southern blot analysis with 3′ and Neo probes, revealing that three of these clones were positive for the correct targeting event. The three positive ES cell clones were independently microinjected into C57Black/6J mouse blastocysts, which were then transferred into pseudopregnant NMRI females. This generated 12 chimeric mice based on coat color. Male chimeras were then mated to C57Black/6J mice, and evidence of germ-line transmission was monitored by *agouti* coat color contributed from the 129Sv-derived ES cell genome.

Males and females with different genotypes were intercrossed to obtain $\alpha_{1D}^{+/+}$, $\alpha_{1D}^{+/-}$, and $\alpha_{1D}^{-/-}$ progeny. Mice were screened by genotyping using Southern blot analysis and PCR for α_{1D}-AR gene. All mice analyzed were from F_3 to F_5, which carried the genetic background of 129Sv and C57Black/6J strains, and $\alpha_{1D}^{+/+}$ littermates were used for analysis as the wild-type mice. Since cardiovascular physiology could differ depending on the difference of mouse strains (22), mice with the same genetic background were always compared as the wild-type. Animals were housed in microisolator cages in a pathogen-free barrier facility. All experimentation was performed under approved institutional guidelines.

RT-PCR analysis. Total RNA from different mouse tissues was prepared using Isogen (Nippon Gene Co. Ltd., Tokyo, Japan). Total RNA (5 μg) was treated with RNase-free DNase (TaKaRa Shuzo Co., Tokyo, Japan) and reverse-transcribed using random hexamers, as described (23). One-tenth of each cDNA sample was amplified by PCR with a receptor-specific primer set and a primer set specific for GAPDH (24). Each sample contained the upstream and downstream primers (10 pmol of each), 0.25 mM of each dNTP, 50 mM KCl, 10 mM Tris-HCl, pH 8.6, 1.5 mM $MgCl_2$, and 2.5 U of *Taq* DNA polymerase (TaKaRa Shuzo Co.). Thermal cycling was performed for 1 minute at 94°C, 1 minute at 56°C, and 2 minutes at 72°C for 27 cycles. The upstream and downstream primers (5′→3′) were AGGCTGCTCAAGTTTTCTCG and CAGATTGGTCCTTTGGCACT for α_{1A} (275 bp), GGGAGAGTTGAAAGATGCCA and TTGGTACTGCTGAGGGTGTC for α_{1B} (752 bp), and CGCTGTGGTGGGAACCGGCAG and ACAGCTGCACTCAGTAGCA-GGTCA for α_{1D} (282 bp). The upstream primer for the α_{1A}-AR or the α_{1B}-AR gene was located within the first exon, and the downstream primer for the α_{1A}-AR or the α_{1B}-AR gene was located within the second exon. The primers for the α_{1D}-AR gene were located within the first exon, and the forward primer was within the region replaced with the Neo in the mutant allele. The primers were derived from the murine α_{1A} (25), α_{1B} (25), and α_{1D} (19, 25) sequences. The GAPDH primers (5′→3′) were GGTCATCATCTCCGCCCCTTC upstream and CCACCACCCTGTTGCTGTAG downstream (662 bp). Control PCR reactions also were performed on non–reverse-transcribed RNA to exclude any contamination by genomic DNA. The amplified DNAs were analyzed on a 1.5% agarose gel with 100 bp DNA marker (New England Biolabs Inc., Beverly, Massachusetts, USA). The specificity of the amplified DNA fragments was determined by Southern blot analysis using receptor-specific ^{32}P-labeled probes (cDNAs of the murine α_{1A}-AR, α_{1B}-AR, and α_{1D}-AR; ref. 25).

TaqMan assay. For rigorous quantification of RT-PCR products, the TaqMan 5′ nuclease fluorogenic quantitative PCR assay was conducted according to manufacturer's instructions, using total RNA from the brain of the $\alpha_{1D}^{+/+}$, $\alpha_{1D}^{+/-}$, and $\alpha_{1D}^{-/-}$ mice. The cDNAs were synthesized from total RNA (5 μg), as described above. TaqMan assays (Applied Biosystems Japan Ltd., Tokyo, Japan) were then carried out using the following oligonucleotides (5′→3′): α_{1D} forward primer CGCTGTGGTGGGAACCGGCAG, α_{1D} reverse primer AGTTGGTGACCGTCTGCAAGT, α_{1D} probe 6FAM-CGGGCAACCTTCTCGTCATCCTCTC-TAMRA, α_{1A} forward primer GCGGTGGACGTCTTATGCT, α_{1A} reverse primer TCACACCAATGTATCGGTCGA, α_{1A} probe 6FAM-CCATCATGGGCCCTGCATCATCT-TAMRA, α_{1B} forward primer CCTGGTCATGTACTGCCGA, α_{1B} reverse primer GACTCCCGCCTCCAGATTC, α_{1B} probe 6FAM-TCTACATCGTGGCAAAGAGGACCACC-TAMRA. All primers used for TaqMan assays were derived from the nucleotide sequences within the first exon of each gene.

Ligand binding. Radioligand binding studies were performed on membrane preparations from the monkey kidney COS cell line (COS) transiently expressing each

mouse α_1-AR subtype and on mouse native tissues, as described previously (26). Briefly, whole brain, heart, liver, kidney, and aorta were dissected from mice (8–18 weeks old), placed in a lysis buffer (250 mM sucrose, 5 mM Tris-HCl, and 1 mM $MgCl_2$, pH 7.4), and homogenized with a Polytron homogenizer (Kinematica AG, Littau-Luzern, Switzerland) at 4°C, at speed 7 for 10 seconds. The homogenate was centrifuged at 35,000 *g* for 20 minutes at 4°C. The resulting pellet was resuspended in binding buffer B (50 mM Tris-HCl, 10 mM $MgCl_2$, and 10 mM EGTA, pH 7.4), and was frozen at –80°C until assayed. A membrane preparation of COS cells transiently expressing mouse α_{1A}-, α_{1B}-, or α_{1D}-AR was also used for binding studies. The collected cells were placed in ice-cold buffer A and disrupted in a sonicator (SONIFER 250; Branson Ultrasonics Corp., Danbury, Connecticut, USA) at setting 5 for 8 seconds. They were then centrifuged at 3,000 *g* at 4°C for 10 minutes to remove the nuclei. The supernatant fraction was centrifuged at 35,000 *g* for 20 minutes at 4°C. Protein concentration was measured using the bicinchoninic acid protein assay kit (Pierce Chemical Co., Rockford, Illinois, USA). Radioligand binding was measured using [^{125}I]-HEAT (^{125}I-(2-b-(4-hydroxyphenyl)-ethylaminomethyl)-tetralone; specific activity, 2,200 Ci/mmol; NEN Life Science Products Inc., Boston, Massachusetts, USA), as described (26). Briefly, measurement of specific [^{125}I]-HEAT binding was performed by incubating 0.1 ml membrane preparation (~1–5 μg protein for COS cell membranes and ~30–200 μg for native tissues), with [^{125}I]-HEAT for 45 minutes at 25°C in the presence or absence of competing drugs. For competition curve analysis, each assay contained about 100 pM [^{125}I]-HEAT. Nonspecific binding was defined as binding displaced by phentolamine (10 μM).

Heart/body weight ratio. Age-matched (3–5 months) $\alpha_{1D}^{+/+}$ or $\alpha_{1D}^{-/-}$ male mice were anesthetized with lethal doses of pentobarbital (200 mg/kg intraperitoneally). The mice were weighed, then their hearts were excised, blotted three times on filter paper, and weighed. Heart/body-weight ratios were calculated and expressed as milligrams per gram.

Histological analysis. Heart and thoracic aorta from $\alpha_{1D}^{+/+}$ or $\alpha_{1D}^{-/-}$ male mice (12–18 weeks old) were perfusion fixed in PBS plus 10% formalin. Several sections of hearts and aorta were obtained for gross morphological analysis, then paraffin embedded for thin sectioning followed by hematoxylin and eosin staining.

Measurement of blood pressure. Systolic blood pressure (SBP) and heart rate (HR) were measured in conscious 12- to 18-week-old male mice (mean body weights were 32.8 g for $\alpha_{1D}^{+/+}$ and 30.1 g for $\alpha_{1D}^{-/-}$ mice, respectively) with a computerized tail-cuff system (BA-98A system; Softron Co., Tokyo, Japan) that determines systolic blood pressure using a photoelectric sensor as described (27). Before the study was initiated, at least 3 days of training sessions (that is, sessions of unrecorded measurements) were provided for the mice to become accustomed to the tail-cuff procedure. Sessions of recorded measurements were then made from 1:00 to 5:00 P.M. daily on 3 consecutive days. Each session included more than ten tail-cuff measurements so that a total of 30–50 measurements were used for the determination of the blood pressure and HR of each mouse. For inclusion of each set of measurements for an individual mouse, we required that the computer successfully identify a blood pressure in at least seven of the ten trials within the set.

Mean arterial blood pressure (MAP) and HR were also measured in nonanesthetized 12- to 18-week-old male mice (mean body weights were 28.8 g for $\alpha_{1D}^{+/+}$ and 28.9 g for $\alpha_{1D}^{-/-}$ mice, respectively) (28). After a cervical incision was made on mice anesthetized with sodium pentobarbital (40 mg/kg, intraperitoneally), a stretched Intramedic PE10 polyethylene catheter (Clay Adams, Parsippany, New Jersey, USA) was inserted into the right carotid artery. The catheter was tunneled through the neck and then placed in a subcutaneous pouch in the back. After a minimum 24-hour recovery, mice were placed in Plexiglas tubes to partially restrict their movements, the saline-filled catheter was removed from the pouch and connected to a pressure transducer (DX-360; Nihon Kohden Corp., Tokyo, Japan) and MAP was recorded on a thermal pen recorder (RTA-1200; Nihon Kohden Corp.). Measurement of HR was triggered from changes in MAP (AT-601G; Nihon Kohden Corp.). To examine pressor responses in unanesthetized mice, drugs in approximately 30 μl of injection volume (1 μl/g of mouse body weight) were administered through the catheter inserted into the right femoral vein as a bolus at 15- to 20-minute intervals after ensuring MAP and HR had returned to baseline levels.

In some experiments, the effect of α_1-antagonists on the norepinephrine-induced pressor response was examined in male mice (10–12 weeks old) anesthetized with sodium pentobarbital (40 mg/kg, intraperitoneally). Following propranolol (1 mg/kg) treatment, either bunazosin hydrochloride (10 μg/kg, intravenously; Eisai Co., Tokyo, Japan) or BMY7378 (100 μg/kg, intravenously; Research Biochemicals International, Natick, Massachusetts, USA) was administered 10 minutes prior to the continuous infusion of norepinephrine (1 μg/kg/min intravenously for 10 minutes) using a microsyringe pump (CFV-2100; Nihon Kohden Corp.).

Echocardiography. Quantitative echocardiographic measurements were performed on lightly anesthetized, spontaneously breathing mice according to a previously published transthoracic method (29). The male mice (12–18 weeks old) were anesthetized (40 mg/kg pentobarbital, intraperitoneally), the chest area was shaved, and ultrasonic gel was applied. The measurements with the SONOS-5500 system (Philips Medical Systems, Andover, Massachusetts, USA) employed a dynamically focused symmetrical annular array transducer (12.5 MHz) for two-dimensional, M-mode, and Doppler imaging. The parasternal long and short axes and four chamber views were visualized. For

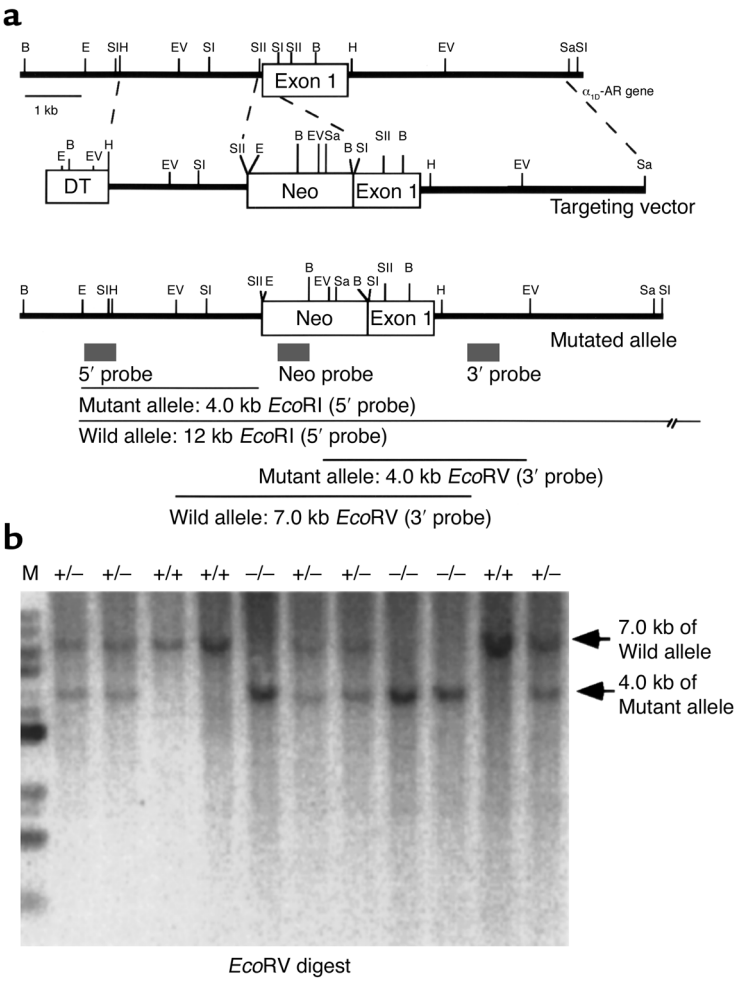

Figure 1
Generation of α_{1D}-AR–deficient mice. (**a**) Simplified restriction map around exon 1 of the α_{1D}-AR gene and structure of the targeting vector. The coding region of the exon is boxed. Neo, PGK-neo cassette; DT, diphtheria toxin-A fragment gene; B, *Bam*HI; E, *Eco*RI; EV, *Eco*RV; H, *Hind*III; Sa, *Sal*I; SI, *Sac*I; SII, *Sac*II. (**b**) Southern blot analysis of tail DNA. DNA was digested with *Eco*RV, and the blot was hybridized with the 3′ probe shown in **a**. The 7-kb band is derived from the wild-type allele (wild) and the 4-kb band from the targeted allele (mutant).

quantitative analysis, measurements were performed in three to five consecutive cardiac cycles. Cardiac parameters determined include interventricular septal thickness (IVS), posterior wall thickness (PW), left ventricular internal dimension in diastole (LVIDd) and in systole (LVIDs), and heart rate (HR). IVS, PW, LVIDd, and LVIDs were normalized to body weight, and percentage of fractional shortening (%FS) was calculated as $100 \times [(\text{LVIDd} - \text{LVIDs})/\text{LVIDd}]$. Cardiac output (CO) was calculated from Doppler echocardiography using the following equation, $[\pi \times (\text{Ao})^2 \times \text{VTI} \times \text{HR}]/4$, where Ao was the diameter of the aortic artery, VTI was the Doppler velocity time integral in left ventricular outflow, and HR was determined from the simultaneous monitoring of electrocardiograms.

Measurement of aortic contraction. The thoracic aorta was excised from mice (12–18 weeks old), cleaned, and cut into 1-mm-long segments. These segments were suspended in isolated tissue baths filled with 10 ml Krebs-Henseleit bicarbonate buffer containing timolol (3 μM), continuously bubbled with a gas mixture of 5% CO_2/95%O_2 at 37°C. One end of the aortic segment was connected to a tissue holder and the other to an isometric force transducer. Aortic segments were equilibrated for 60 minutes under a resting tension of 0.5 *g*, and the buffer was replaced every 15 minutes. In a preliminary experiment, the length of the smooth muscle was increased stepwise during the equilibration period to adjust passive wall tension to 0.5 *g*; this resting tension was found to be optimal for KCl-induced (40 mM) aortic contraction of mice weighing 22–28 g. Care was taken to avoid endothelial damage; functional integrity of the endothelium was assessed using acetylcholine (10 μM). Only intact segments were used for further analysis.

Pressor response in perfused mesenteric arterial beds. The perfused mesenteric arterial bed was prepared according to the methods described previously (30). The superior mesenteric artery of diethylether-anesthetized mice (12–18 weeks old) was dissected, and a stainless-steel cannula (27G syringe) was inserted. The preparations were perfused with Krebs-Henseleit solution equilibrated with a mixture of 95% O_2 and 5% CO_2 (PO_2 > 600 mmHg). The entire ileum was dissected longitudinally at the opposite site of mesenteric vasculature. The preparation was placed in a chamber with a warm water jacket to maintain the temperature at 37°C. The perfusion flow rate was maintained at 1.0 ml/min using a peristaltic pump. Perfusion pressure was measured through a branch of the perfusion cannula by means of a pressure transducer (TP-400T; Nihon Kohden Corp.) connected to a carrier amplifier (AP-621G; Nihon Kohden Corp.) and recorded on a thermal pen recorder (WT-645G; Nihon Kohden Corp.). The preparations were equilibrated for 30 minutes before administration of phenylephrine.

Measurement of serum catecholamines. After 1 hour of stable anesthesia (80 mg/kg pentobarbital, intraperitoneally), an abdominal incision was made, and blood samples were obtained from mice (12–18 weeks old) by venipuncture of the vena cava. Total plasma catecholamine levels (epinephrine, norepinephrine, and dopamine) were determined in 200 μl of plasma samples by HPLC using commercially available reagents (Tosho Co., Tokyo, Japan).

Statistics. All values are expressed as means plus or minus SEM. Statistical analysis was performed using two-way ANOVA. A *P* value less than 0.05 by a Student *t* test was considered statistically significant. Competi-

tion data from the radioligand binding study were analyzed using the iterative nonlinear regression program, LIGAND (31). The presence of one, two, or three different binding sites was assessed using the *F* test in the program. The model adopted was that which provided the significant best fit ($P < 0.05$).

Results

Targeted disruption of the mouse α_{1D}-AR gene. The strategy for inactivating one copy of the α_{1D}-AR gene in ES cells is described in Figure 1a. Homologous recombinants were identified by Southern blot analysis of genomic DNA. Three of the positive ES clones confirmed by Southern blot analysis with the 5′, 3′, and Neo probe were independently microinjected into C57Black/6J blastocyst-stage embryos. Five of 12 chimeric mice were mated to C57Black/6J mice, and germline transmission of the mutant allele was confirmed by genomic Southern analysis of tail DNA from F_1 progeny. Mating between heterozygous male and female mice generated F_2 progeny with all three genotypes: homozygous mutant, heterozygous mutant, and wild-type mice (Figure 1b). The wild-type allele generates a 7-kb *Eco*RV fragment, and the mutant allele generates a 4-kb *Eco*RV fragment. Analysis of the α_{1D}-AR genotype frequencies after intercrosses of heterozygous mutant mice did not reveal any deviation from Mendelian expectations ($\alpha_{1D}^{+/+}$ 30%, $\alpha_{1D}^{+/-}$ 44%, $\alpha_{1D}^{-/-}$ 26%, $n = 212$). Monitoring of mice body weight at 4 weeks old did not reveal any significant difference in growth among mice of different α_{1D}-AR genotypes

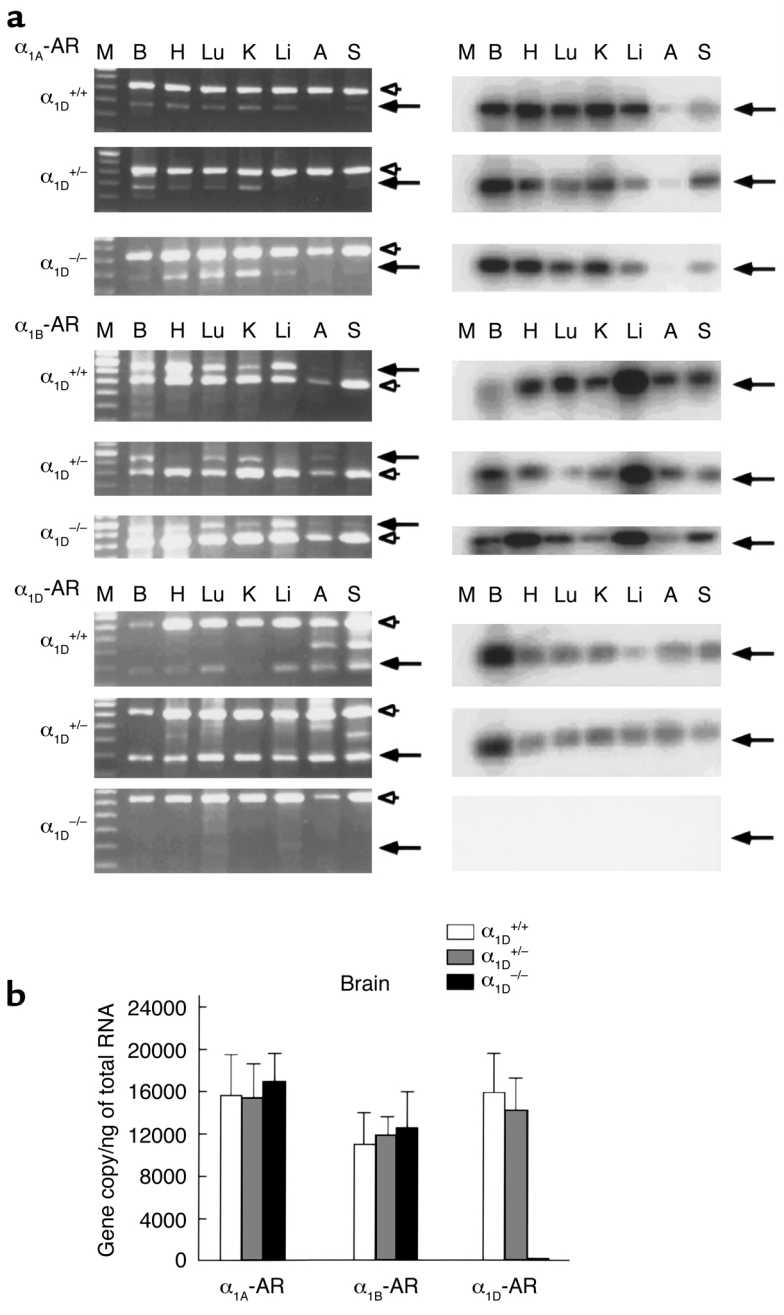

Figure 2
RT-PCR analysis of the RNA from tissues of $\alpha_{1D}^{+/+}$, $\alpha_{1D}^{+/-}$, and $\alpha_{1D}^{-/-}$. (**a**) Ethidium bromide staining of RT-PCR fragments (left). The α_{1A}-, α_{1B}-, and α_{1D}-AR mRNA transcripts were detected and are shown in the upper, middle, and lower panels as 275-, 752-, and 282-bp fragments, respectively, indicated by the arrows. RT-PCR analysis was controlled by detection of the 662-bp fragment of GAPDH message, indicated by the arrowhead. Southern blots of the RT-PCR fragments are shown on the right. The specificity of the amplified fragments was assessed using ^{32}P-labeled probes specific for each receptor subtype. M, 100-bp DNA marker; B, Brain; H, Heart; Lu, Lung; K, Kidney; Li, Liver; A, Aorta; S, Spleen. (**b**) TaqMan assay. Total RNA was isolated from whole brain and reverse-transcribed. Relative RNA levels of each α_1-AR subtype, standardized against GAPDH levels, were obtained by semiquantitative PCR using the TaqMan system. Values represent the mean ± SEM of five independent experiments.

Table 1
Ligand binding in tissues of mutant mice

	B_{max} (fmol/mg protein)	
Tissue	$\alpha_{1D}^{+/+}$	$\alpha_{1D}^{-/-}$
Whole brain	101.2 ± 6.6	92.2 ± 1.7[A]
Cerebral cortex	247.0 ± 23.2	153.0 ± 30.6[A]
Aorta	47.1 ± 13.0	ND
Heart	47.9 ± 7.5	43.8 ± 7.7
Kidney	30.2 ± 1.3	31.5 ± 1.9

Each value is the mean ± SEM of five to eight different experiments. [A]$P < 0.05$ as compared to $\alpha_{1D}^{+/+}$ mice in a paired two-tailed t test. ND, not detected.

(16.2 ± 2.1 g, $n = 20$, and 16.8 ± 2.5 g, $n = 25$, for male $\alpha_{1D}^{+/+}$ and $\alpha_{1D}^{-/-}$, respectively; 14.6 ± 1.9 g, $n = 23$, and 13.8 ± 2.2 g, $n = 21$, for female $\alpha_{1D}^{+/+}$ and $\alpha_{1D}^{-/-}$, respectively). Thus, disruption of the α_{1D}-AR gene does not seem to have any major effect on mouse development, fertility, growth, or feeding behavior under standard breeding conditions.

mRNA expression of the α_1-AR subtypes. Because of the low abundance of the mRNA levels for different α_1-AR subtypes in various animal species (12), RT-PCR was used to assess the expression of α_{1A}-, α_{1B}-, and α_{1D}-ARs in various tissues from male $\alpha_{1D}^{+/+}$, $\alpha_{1D}^{+/-}$, and $\alpha_{1D}^{-/-}$ mice. As shown in Figure 2, in $\alpha_{1D}^{+/+}$ and $\alpha_{1D}^{+/-}$ mice, the α_{1D}-AR was expressed in all tissues examined. On the other hand, no α_{1D}-AR transcript was detectable in the $\alpha_{1D}^{-/-}$ mice, while α_{1A}- and α_{1B}-AR were detected in all tissues tested (Figure 2). Thus, we confirmed that the knockout of the α_{1D}-AR gene was successful by RT-PCR using the upstream primer within the deleted region and the downstream primer located within the first exon. With other primer set within the second exon of the α_{1D}-AR gene (the upstream primer: 5′-TTCC-CTCAGCTGAAACCATCA-3′, and the downstream primer: 5′-CCTGGGTGTGCAGTGAGGGCT-3′), however, a faint band of the α_{1D}-AR gene was detected by Southern blot analysis, suggesting that an aberrant mRNA could be transcribed from the mutant allele (data not shown).

To investigate potential compensatory changes in expression of other α_1-AR subtypes for loss of α_{1D}-AR in $\alpha_{1D}^{-/-}$ mice, we further examined changes in α_1-AR transcription in the brain (where all three α_1-AR subtypes are expressed) using a more rigorous quantitative RT-PCR analysis, the TaqMan assay. As summarized in Figure 2b, no α_{1D}-AR transcript was detectable in the $\alpha_{1D}^{-/-}$ mice, but expression of α_{1A}- and α_{1B}-ARs was similar to that in $\alpha_{1D}^{+/+}$ or $\alpha_{1D}^{+/-}$ mice, suggesting that inactivation of the α_{1D}-AR gene does not lead to any dramatic compensatory change in expression of the other subtypes.

Radioligand binding studies. Saturation binding analysis showed that the K_d value for the α_1-antagonist [^{125}I]-HEAT was approximately 100 pM in the tissues examined from both $\alpha_{1D}^{+/+}$ and $\alpha_{1D}^{-/-}$ mice (data not shown). On the other hand, receptor density (B_{max}) was significantly reduced by 10–40% in whole brain and cerebral cortex and was not detected in the aorta of the $\alpha_{1D}^{-/-}$ mice. However, no significant decrease in B_{max} was observed in heart and kidney (Table 1).

To better assess the expression of different α_1-AR subtypes, competition binding experiments using the α_{1D}-AR–selective antagonist BMY7378 were further performed in the aorta and brain (cortex and hippocampus) of $\alpha_{1D}^{+/+}$ and $\alpha_{1D}^{-/-}$ mice. Nonlinear regression analysis using LIGAND showed that inhibition curves for BMY7378 in the aorta of the $\alpha_{1D}^{+/+}$ mice best fit a one-site model with a high-affinity competition curve ($P < 0.05$ vs. a two-site model). This strongly suggests a large prevalence of the α_{1D}-AR in this tissue. On the other hand, inhibition curves for BMY7378 in the cortex and hippocampus of the $\alpha_{1D}^{+/+}$ mice best fit a two-site model ($P < 0.05$ vs. a one-site model), suggesting coexistence of the α_{1D}-AR and one or other subtypes in these tissues (Table 2). As shown in Table 2, a selective decrease in the high-affinity sites in cerebral cortex and hippocampus in the $\alpha_{1D}^{-/-}$ mice reflects loss of α_{1D}-AR. On the other hand, the remaining low-affinity binding sites in both cerebral cortex and hippocampus of the $\alpha_{1D}^{-/-}$ mice might reflect the presence of the α_{1A}-AR and/or α_{1B}-AR in these tissues. The affinity estimates of BMY7378 for native α_1-ARs were confirmed to be comparable to those obtained for cloned mouse α_1-ARs; thus, BMY7378 displayed high affinity (inhibition constant [K_i] = 5.5 ± 0.8 nM, $n = 6$) for the

Table 2
Interaction of BMY7378 with α_1-AR–binding sites in membrane preparations from mouse tissues

		Two-site analysis				
Mouse	Tissue	K_H (nM)	K_L (nM)	R_H (%)	R_L (%)	P value
$\alpha_{1D}^{+/+}$	Whole brain		149 ± 20	0	100	
	Cerebral cortex	0.7 ±0 .1	342 ± 50.5	11 ± 2	89 ± 13	<0.05
	Hippocampus	2.8 ± 0.1	814 ± 79.9	24 ± 2	76 ± 9	<0.05
	Aorta	0.4 ± 0.2		100	0	
$\alpha_{1D}^{-/-}$	Cerebral cortex		304 ± 37.9	0	100	
	Hippocampus		423 ± 122	0	100	

Inhibition of specific [^{125}I]HEAT binding by BMY7378 was determined in membrane preparations from each tissue, as described. The best two-site fit was determined by nonlinear regression analysis of the averaged curve, and high-affinity (R_H) and low-affinity (R_L) sites for BMY7378 were determined as described. K_H, K_i value at high-affinity site. K_L, K_i value at low-affinity site. The P value for the best two-site fit compared with the best one-site fit is given. Each value is the mean ± SEM of six different experiments.

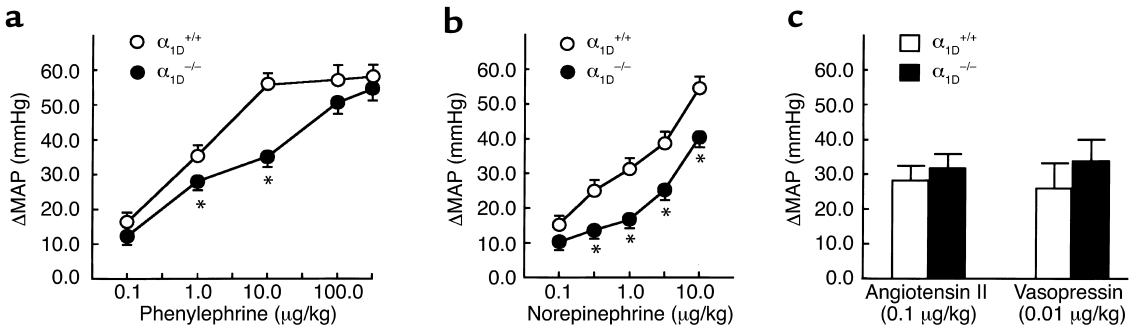

Figure 3
Blood pressure responses in $\alpha_{1D}^{+/+}$ and $\alpha_{1D}^{-/-}$ mice. Phenylephrine (**a**), norepinephrine (**b**), angiotensin II or vasopressin (**c**) was injected intravenously as a bolus to male nonanesthetized $\alpha_{1D}^{+/+}$ (open circles, n = 8) or $\alpha_{1D}^{-/-}$ mice (filled circles, n = 12) (12–18 weeks old). The effects on blood pressure are shown and expressed as the change in MAP (in mmHg). Responses to phenylephrine or norepinephrine in $\alpha_{1D}^{-/-}$ mice were significantly decreased at doses as indicated compared with the wild-type response. The maximal increase in blood pressure is shown. Points represent the mean ± SEM. *P < 0.05 as compared with $\alpha_{1D}^{+/+}$ mice.

mouse α_{1D}-AR expressed in COS-7 cells (K_i values for mouse α_{1A}- and α_{1B}-ARs were 490 ± 30 nM and 410 ± 5 nM, n = 6 each, respectively). Competition binding studies with other α_1-antagonists (prazosin or the α_{1A}-AR–selective antagonist KMD-3213) showed no difference in their affinities between $\alpha_{1D}^{+/+}$ and $\alpha_{1D}^{-/-}$ mice, indicating that the remaining α_{1A}- and α_{1B}-ARs were not much changed with respect to their pharmacological properties (data not shown).

Heart weight and histological analysis. Heart-weight/body-weight ratio did not significantly differ between $\alpha_{1D}^{+/+}$ and $\alpha_{1D}^{-/-}$ mice (4.96 ± 0.31 mg/g, n = 10, and 5.22 ± 0.24 mg/g, n = 14, in $\alpha_{1D}^{+/+}$ and $\alpha_{1D}^{-/-}$, respectively). There were no obvious differences between $\alpha_{1D}^{+/+}$ and $\alpha_{1D}^{-/-}$ mice with respect to gross morphology or microscopic myocyte appearance of hearts and aorta (data not shown).

Measurement of blood pressure. The HR and blood pressure were analyzed in male mice 12–18 weeks of age. The resting SBP, measured by tail-cuff reading or MAP, measured by direct intra-arterial recording under unanesthetized conditions, were significantly (P < 0.05) lower in $\alpha_{1D}^{-/-}$ mice compared with $\alpha_{1D}^{+/+}$ mice (SBP: 108.7 ± 1.9 mmHg, n = 31, and 99.1 ± 1.7 mmHg, n = 23, in $\alpha_{1D}^{+/+}$ and $\alpha_{1D}^{-/-}$, respectively; MAP: 116.5 ± 2.2 mmHg, n = 14, and 106.9 ± 3.7 mmHg, n = 18, in $\alpha_{1D}^{+/+}$ and $\alpha_{1D}^{-/-}$, respectively); however, there was no significant difference in HR in beats per minute (bpm) between the two groups monitored by either tail-cuff reading or the intra-arterial measurements (554 ± 13 bpm, n = 31, and 529 ± 13 bpm, n = 23, by tail cuff reading in $\alpha_{1D}^{+/+}$ and $\alpha_{1D}^{-/-}$, respectively; 616 ± 12 bpm, n = 14, and 638 ± 17 bpm, n = 18, by intra-arterial measurements in $\alpha_{1D}^{+/+}$ and $\alpha_{1D}^{-/-}$, respectively).

We next examined the pressor responses to several vasoactive agents in nonanesthetized mice. Increasing doses of phenylephrine or norepinephrine progressively increased the blood pressure in both $\alpha_{1D}^{+/+}$ and $\alpha_{1D}^{-/-}$ mice. As shown in Figure 3, a and b, these pressor responses were considerably reduced in the $\alpha_{1D}^{-/-}$ as compared with the $\alpha_{1D}^{+/+}$ mice; however, the pressor responses caused by higher doses of phenylephrine (> 100 μg/kg) were not significantly different. The final absolute blood pressures at maximum dose of norepinephrine (10 μg/kg) in $\alpha_{1D}^{+/+}$ (n = 8) and $\alpha_{1D}^{-/-}$ (n = 12) were 163.0 ± 2.5 mmHg and 145.5 ± 4.1 mmHg, respectively, and those at maximum dose of phenylephrine (300 μg/kg) were 166.0 ± 3.7 mmHg and 162.0 ± 3.8 mmHg, respectively.

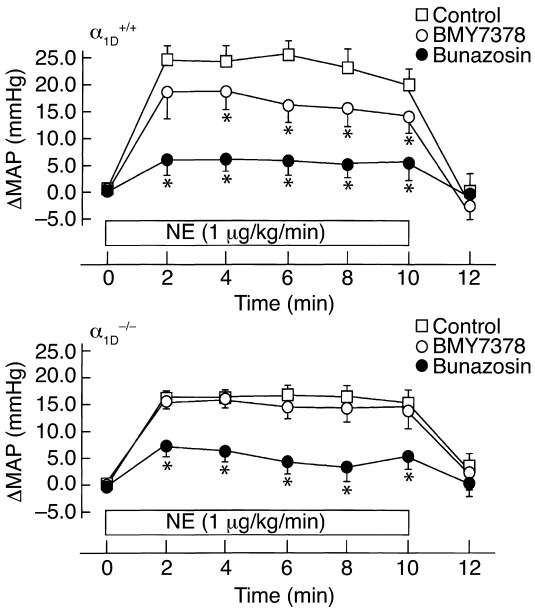

Figure 4
Effects of BMY7378 or bunazosin on blood pressure responses in $\alpha_{1D}^{+/+}$ and $\alpha_{1D}^{-/-}$ mice under anesthesia. Inhibitory effects of BMY7378 or bunazosin on the pressor response to norepinephrine in $\alpha_{1D}^{+/+}$ (upper) and $\alpha_{1D}^{-/-}$ (lower) mice. β-Blocker, propranolol (1 mg/kg) was preadministered, and BMY7378 (100 μg/kg) or bunazosin (10 μg/kg) was injected into male $\alpha_{1D}^{+/+}$ or $\alpha_{1D}^{-/-}$ mice (10–12 weeks old) 10 minutes prior to continuous infusion of norepinephrine (1 μg/kg/min, for 10 minutes). Points represent the mean ± SEM of eight mice. Open squares, norepinephrine infusion; open circles, norepinephrine infusion + BMY7378 pretreatment; filled circles, norepinephrine infusion + bunazosin pretreatment. *P < 0.05 as compared with norepinephrine infusion.

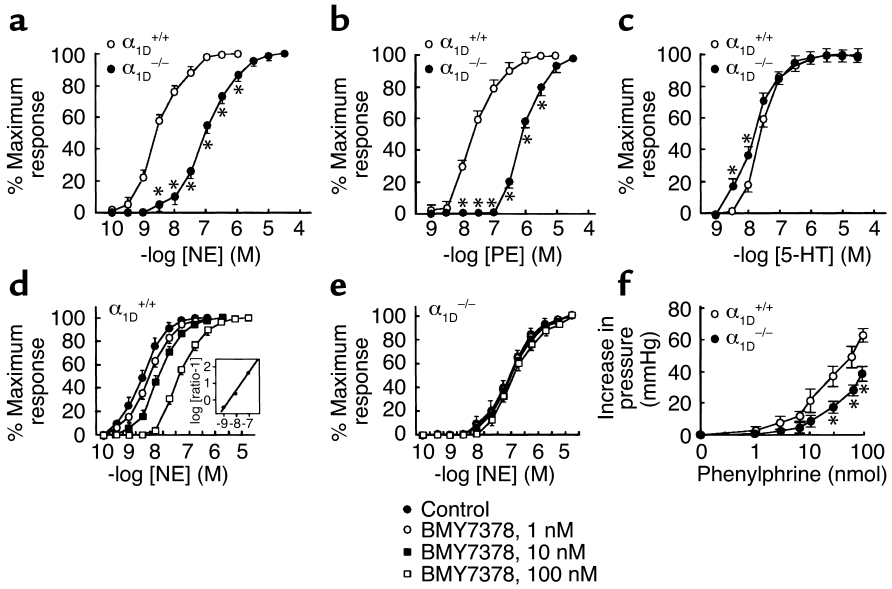

Figure 5

Vascular contraction in $\alpha_{1D}^{+/+}$ and $\alpha_{1D}^{-/-}$ mice. The contractile response to norepinephrine (NE), phenylephrine (PE), and serotonin (5-HT). Concentration-response curves for norepinephrine-induced (**a**), phenylephrine-induced (**b**), and serotonin-induced contractions (**c**) in aortic segments from $\alpha_{1D}^{-/-}$ (filled circles) or $\alpha_{1D}^{+/+}$ mice (open circles). The results are the mean ± SEM of 15–27 preparations for NE, PE, or 5-HT. Effects of BMY7378 on norepinephrine-induced contractions in aortic segments of $\alpha_{1D}^{+/+}$ (**d**) or $\alpha_{1D}^{-/-}$ mice (**e**). Aortic segments were exposed to vehicle (filled circles, control) or different concentrations of BMY7378 (open circle, 1 nM; filled squares, 10 nM; open squares, 100 nM), prior to the addition of cumulative concentrations of norepinephrine (NE). Inset (**d**): A Schild plot derived from the data from $\alpha_{1D}^{+/+}$ mice was fitted by a straight line (R^2 = 0.92) with a slope of 1.06 ± 0.11. Data represent the mean ± SEM of six different aortic segments for each group. (**f**) Concentration-response curves for phenylephrine-induced pressor response in perfused mesenteric arterial beds of $\alpha_{1D}^{-/-}$ mice (filled circles, n = 9) or $\alpha_{1D}^{+/+}$ (open circles, n = 7). Two-way ANOVA showed that concentration-response curve for phenylephrine-induced pressor response of $\alpha_{1D}^{-/-}$ mice was significantly (P < 0.05) different from that of the $\alpha_{1D}^{+/+}$ mice. *P < 0.05 as compared with $\alpha_{1D}^{+/+}$.

The maximal plateau level of pressor responses by norepinephrine was not successfully monitored, because administration of higher doses of norepinephrine frequently caused circulatory collapse, probably due to its cardiac toxicity. Despite the diminished response to phenylephrine and norepinephrine in the $\alpha_{1D}^{-/-}$ mice, the increase in blood pressure induced by angiotensin II (0.1 μg/kg) or vasopressin (0.01 μg/kg) did not significantly differ between the $\alpha_{1D}^{+/+}$ and $\alpha_{1D}^{-/-}$ mice (Figure 3c).

The contribution of the α_{1D}-AR to the α_1-AR–mediated pressor response was further assessed in anesthetized mice. As shown in Figure 4, continuous infusion of norepinephrine (1 μg/kg/min, 10 minutes) promptly induced a significant blood pressure increase that lasted for 10 minutes. The increase in MAP was approximately 25 mmHg in $\alpha_{1D}^{+/+}$ mice, while it was significantly lower in $\alpha_{1D}^{-/-}$ mice (~17 mmHg) (Figure 4). Pretreatment with BMY7378 (100 μg/kg) significantly inhibited the norepinephrine-induced pressor response in $\alpha_{1D}^{+/+}$ mice, while it had no effect in $\alpha_{1D}^{-/-}$ mice (Figure 4). Pretreatment with the nonselective α_1-antagonist bunazosin (10 μg/kg), on the other hand, more strongly inhibited the norepinephrine-induced pressor response in both $\alpha_{1D}^{+/+}$ and $\alpha_{1D}^{-/-}$ mice (Figure 4).

Cardiac function. The cardiac output (CO) was similar in the $\alpha_{1D}^{-/-}$ and control mice (18.6 ± 1.6 ml/min, n = 15, and 16.3 ± 1.2 ml/min, n = 18, in $\alpha_{1D}^{+/+}$ and $\alpha_{1D}^{-/-}$, respectively). Myocardial contractility monitored with %FS also showed no significant difference between the $\alpha_{1D}^{+/+}$ and $\alpha_{1D}^{-/-}$ mice (49.7% ± 2.7%, n = 15, and 49.5% ± 2.1%, n = 18, in $\alpha_{1D}^{+/+}$ and $\alpha_{1D}^{-/-}$, respectively). The left ventricular wall thickness measured at the IVS and PW was similar in the two groups (data not shown). During echocardiography, HRs were similar in the two groups (501 ± 27 bpm, n = 15, and 522 ± 23 bpm, n = 18, in $\alpha_{1D}^{+/+}$ and $\alpha_{1D}^{-/-}$, respectively).

Plasma catecholamines. Total plasma catecholamines were comparable between the two groups of mice (5.5 ± 0.5 ng/ml and 4.8 ± 0.8 ng/ml, n = 10 each, for $\alpha_{1D}^{+/+}$ and $\alpha_{1D}^{-/-}$, respectively).

Vascular contraction. To assess whether α_{1D}-AR was directly involved in vascular smooth muscle contraction, we measured the effect of norepinephrine and phenylephrine on the contraction of isolated aortic segments from male $\alpha_{1D}^{+/+}$ and $\alpha_{1D}^{-/-}$ mice. As shown in Figure 5a, norepinephrine induced concentration-dependent contractile responses in aortic segments from $\alpha_{1D}^{+/+}$ and $\alpha_{1D}^{-/-}$ mice. However, the potency of the response was markedly reduced in aortic segments from $\alpha_{1D}^{-/-}$ as compared with $\alpha_{1D}^{+/+}$ mice (Figure 5a). A similar decrease in potency was also observed with phenylephrine-induced contractile responses (Figure 5b). The EC_{50} values of norepinephrine and phenylephrine were increased approximately 50- and 40-fold in $\alpha_{1D}^{-/-}$ mice compared with $\alpha_{1D}^{+/+}$ mice (50% effective dose [EC_{50}] val-

ues: 3.8 ± 0.5 nM, n = 26, in $\alpha_{1D}^{+/+}$ mice, and 190 ± 40 nM, n = 15, in $\alpha_{1D}^{-/-}$ mice for norepinephrine; 20.0 ± 2.0 nM, n = 27, in $\alpha_{1D}^{+/+}$ mice, and 840 ± 40 nM, n = 15, in $\alpha_{1D}^{-/-}$ mice for phenylephrine, respectively). The contractile response induced by serotonin was not decreased. Rather, the concentration-response curve of serotonin-induced contraction was slightly shifted to the left in $\alpha_{1D}^{-/-}$ mice compared with $\alpha_{1D}^{+/+}$ mice (EC_{50} values: 28.0 ± 2.1 nM in $\alpha_{1D}^{+/+}$ mice and 12.1 ± 2.4 nM in $\alpha_{1D}^{-/-}$ mice, n = 15 each) (Figure 5c).

The contractile response induced by norepinephrine was competitively antagonized by BMY7378 in $\alpha_{1D}^{+/+}$ mice (Figure 5d), but only to a small extent in $\alpha_{1D}^{-/-}$ mice (Figure 5e). Competitive antagonism was shown by Schild analysis in which the negative logarithms of the dissociation constant (pA_2 value) was 8.61 ± 0.2 and the slope was 1.06 ± 0.11 (n = 6) for BMY7378 in $\alpha_{1D}^{+/+}$ mice. This pA_2 value was in good agreement with K_i values (~1 nM) obtained in binding studies with the cloned mouse α_{1D}-AR and aorta.

The contractile response to α_1-AR in aorta was observed to be reduced in $\alpha_{1D}^{-/-}$ mice, clearly showing that α_{1D}-AR mediate aortic contraction; however, aorta is a conduit artery that may not directly control blood pressure. Hence, we further examined the α_1-AR–mediated vascular response in the resistance arteries of mesenteric arterial beds. As shown in Figure 5f, the pressor response of isolated perfused mesenteric arterial beds to phenylephrine was significantly attenuated in $\alpha_{1D}^{-/-}$ compared with $\alpha_{1D}^{+/+}$ mice.

Discussion

Using gene targeting to create a mouse model lacking the α_{1D}-AR, we investigated the functional role of the α_{1D}-AR subtype in the cardiovascular system. By RT-PCR and radioligand binding studies, we confirmed a loss of α_{1D}-AR expression in $\alpha_{1D}^{-/-}$ mice and observed little apparent compensatory upregulation of the other subtypes. The $\alpha_{1D}^{-/-}$ mice showed a modest hypotension under unanesthetized conditions without a notable increase in heart rate. Also, there was no significant alteration in ventricular function or in the circulating catecholamine levels between the $\alpha_{1D}^{-/-}$ and $\alpha_{1D}^{+/+}$ mice. Consistent with the loss of α_{1D}-AR expression, $\alpha_{1D}^{-/-}$ mice showed reduced pressor responses to α_1-AR stimulation, and the contractile responses of the aorta and mesenteric arterial beds to α_1-agonists were markedly suppressed. The present study provides clear evidence that the α_{1D}-AR mediates a pressor response to catecholamines by directly regulating vasoconstriction.

Our study showed that the α_{1D}-AR regulates not only the vasopressor response to α_1-AR stimulation, but also the resting blood pressure. Conscious $\alpha_{1D}^{-/-}$ mice showed a slight but significant decrease in the resting blood pressure measured by the tail-cuff method as well as by direct intra-arterial measurement. Because cardiac outputs assessed by echocardiogram were similar between the $\alpha_{1D}^{-/-}$ and $\alpha_{1D}^{+/+}$ mice, the modest hypotension observed in $\alpha_{1D}^{-/-}$ mice is considered to be mainly due to the reduction in total peripheral resistance. However, an increase in heart rate, an expected compensatory response to a low blood pressure, was not observed in $\alpha_{1D}^{-/-}$ mice. The mechanism for the lack of reflex tachycardia in $\alpha_{1D}^{-/-}$ mice cannot be fully explained from the present study, but interestingly, chronic administration of α_1-AR blocking drugs has been reported to lower blood pressure without causing reflex tachycardia in patients with essential hypertension (32).

Although in vitro as well as in vivo pharmacological studies (33–36) have implicated a predominant role for α_{1D}-AR in the vascular contractions caused by α_1-AR agonists, our present study clearly shows, we believe for the first time, that α_{1D}-ARs directly mediate α_1-AR–stimulated vascular smooth muscle contraction. As shown in RT-PCR and radioligand binding studies, murine aorta predominantly expresses the α_{1D}-AR. Corresponding to the loss of α_{1D}-AR expression, we observed a marked reduction of α_1-AR–stimulated aortic contractile response in $\alpha_{1D}^{-/-}$ mice, showing that α_{1D}-ARs are predominantly responsible for α_1-AR–stimulated aortic contraction. This observation obtained in a conduit artery of aorta, however, may not be directly extrapolated to the resistance vessels in general, because many studies have shown that the dominant contractile α_1-AR varies with vascular bed type (37–40). Hence, we further examined the α_1-AR–mediated vascular response in the resistance artery that more directly controls blood pressure and observed a significant reduced α_1-AR–stimulated pressor response in isolated perfused mesenteric arterial preparation of $\alpha_{1D}^{-/-}$ mice. The results, therefore, show that the α_{1D}-AR contributes to the regulation of not only the conduit-type vasculatures (such as the aorta), but also the muscular-type resistance vessels, which are more responsible for pressor reactivity. Taken together, our functional examinations in $\alpha_{1D}^{-/-}$ mice show that the α_{1D}-AR plays a significant role in direct regulation of peripheral vascular tone. However, pressor response experiments in $\alpha_{1D}^{-/-}$ mice did not completely exclude the possibility that subtypes other than α_{1D}-AR are involved in α_1-AR–stimulated pressor response. In fact, the dose-pressor response for phenylephrine (Figure 3a) showed that the pressor responses in $\alpha_{1D}^{-/-}$ mice were significantly reduced only at the midrange doses, and the pressor responses at maximum doses were comparable to control. These data may indicate not only that α_{1D}-AR is involved in vasopressor response to phenylephrine, but also that other α_1-AR subtypes are involved in vasopressor response.

Our $\alpha_{1D}^{-/-}$ mice showed little adrenergic compensatory effect on α_{1D}-AR at the cardiovascular level. The TaqMan assay and binding study in $\alpha_{1D}^{-/-}$ mice showed that other α_1-AR subtypes are apparently not upregulated to compensate for the loss of α_{1D}-AR. Furthermore, comparison of the inhibitory effects of the nonselective α_1-antagonist bunazosin and the α_{1D}-AR–

selective antagonist BMY7378 on norepinephrine-induced pressor responses in $\alpha_{1D}^{+/+}$ and $\alpha_{1D}^{-/-}$ mice showed little adrenergic compensatory effect; rather, it suggested the contribution of other subtype(s) to the α_1-AR–mediated pressor response. The results clearly show that despite the presence of multiple α_1-AR subtypes in the same tissue, at best there is only partial functional redundancy in cardiovascular tissue (i.e., multiple α_1-AR subtypes can mediate the vasopressor response, but cannot compensate for each other). A similar observation regarding functional redundancy has been made in a study of α_{1B}-AR knockout mice (16). Together with previous observations in α_{1B}-AR knockout mice (16), our study supports the idea that α_{1B}- as well as α_{1D}-ARs contribute to the α_1-AR–mediated pressor response. Moreover, together with information on tissue distribution and from observations in α_{1B}-AR knockout mice (16), our present study would provide further important definition of the role(s) of each α_1-AR subtype in the cardiovascular system. Thus, α_{1D}-ARs may have a specific effect on the vascular system, while having little effect on the heart. The α_{1B}-AR subtype may be linked to both cardiac and vascular effects (16, 41, 42). The α_{1A}-AR, however, may regulate cardiac function, since α_{1A}-AR knockout mice mainly display impaired cardiac function (43). These findings are of particular importance for better understanding of the cardiovascular effects of drugs acting at the α_1-AR and for more precisely defining goals linked to the development of α_1-AR subtype–selective ligands.

Because α_1-AR subtype expression is known to be markedly varied depending on vessel type and species, one must be careful in directly extrapolating findings obtained from knockout mice to human vascular α_1-AR physiology. At present, the distribution of α_1-AR subtypes in blood vessels is relatively well characterized at mRNA or protein levels, but the available information regarding α_1-AR subtypes mediating vasoconstriction is still very scarce in humans (44). Furthermore, in mice, little is known about either the distribution or function of α_1-AR subtypes in blood vessels. Studies have been hampered both by the lack of drugs sufficiently selective for the three subtypes and by cross-reactivity of α_1-AR ligands with other receptors. In fact, the α_{1D}-AR subtype–selective antagonist BMY7378 used in the present study is known to have a broader pharmacological profile (also acting as a 5-HT_{1A} receptor partial agonist). Using $\alpha_{1D}^{-/-}$ mice, however, we showed that BMY7378 is selective for α_{1D}-AR–mediated function. As exemplified in the present study, the knockout mice of each α_1-AR subtype would be of use in developing and evaluating subtype-selective pharmacological agents.

In conclusion, our knockout mouse study has demonstrated the physiological role of α_{1D}-AR in the cardiovascular system; thus, the α_{1D}-AR mediates the pressor response to catecholamines by directly regulating vasoconstriction. Enhanced activity of the α_{1D}-AR has been suggested to be involved in the pathogenesis and/or maintenance of hypertension (45–47) and age-related changes in vascular responsiveness (48) and also other physiological effects, such as vascular smooth muscle cell growth and hypertrophy (49, 50). The α_{1D}-AR knockout mice would be of value in studying mechanisms involved in the control of vascular physiology and its dysregulation. α_1-AR subtype knockout mice (single, double, and triple knockouts) should constitute useful models to clarify the functional specificity of each α_1-AR subtype and provide a valuable experimental platform for assessing and developing new therapeutic agents.

Acknowledgments

We thank M. Narutomi for assistance. This work was supported in part by research grants from the Scientific Fund of the Ministry of Education, Science, and Culture of Japan, the Japan Health Science Foundation and Ministry of Human Health and Welfare, the Organization for Pharmaceutical Safety and Research (OPSR), and a Grant for Liberal Harmonious Research Promotion System from the Science and Technology Agency.

1. Hoffman, B.B., and Lefkowitz, R.J. 1996. Catecholamines, sympathomimetic drugs, and adrenergic receptor antagonists. In *The pharmacological basis of the therapeutics*. J.G. Hardman, E. Limbird, L.P.B. Molinoff, and R.W. Ruddon, editors. McGraw-Hill. New York, New York, USA. 199–248.
2. Cotecchia, S., et al. 1988. Molecular cloning and expression of the cDNA for the hamster α_1-adrenergic receptor. *Proc. Natl. Acad. Sci. USA.* **85**:7159–7163.
3. Schwinn, D.A., et al. 1990. Molecular cloning and expression of the cDNA for a novel α_1-adrenergic receptor subtype. *J. Biol. Chem.* **265**:8183–8189.
4. Perez, D.M., Piascik, M.T., and Graham, R.M. 1991. Solution-phase library screening for the identification of rare clones: isolation of an α_{1D}-adrenergic receptor cDNA. *Mol. Pharmacol.* **40**:876–883.
5. Hirasawa, A., et al. 1993. Cloning, functional expression and tissue distribution of human cDNA for the α_{1C}-adrenergic receptor. *Biochem. Biophys. Res. Commun.* **195**:902–909.
6. Esbenshade, T.A., et al. 1995. Cloning of the human α_{1d}-adrenergic receptor and inducible expression of three human subtypes in SK-N-MC cells. *Mol. Pharmacol.* **47**:977–985.
7. Hieble, J.P., et al. 1995. International Union of Pharmacology. X. Recommendation for nomenclature of α_1-adrenoceptors: consensus update. *Pharmacol. Rev.* **47**:267–270.
8. McGrath, J.C. 1982. Evidence for more than one type of post-junctional α_1-adrenoceptor. *Biochem. Pharmacol.* **31**:467–484.
9. Han, C., Abel, P.W., and Minneman, K.P. 1987. α_1-adrenoceptor subtypes linked to different mechanisms for increasing intracellular Ca^{2+} in smooth muscle. *Nature.* **329**:333–335.
10. Foglar, R., Shibata, K., Horie, K., Hirasawa, A., and Tsujimoto, G. 1995. Use of recombinant α_1-adrenoceptors to characterize subtype selectivity of drugs for the treatment of prostatic hypertrophy. *Eur. J. Pharmacol.* **288**:201–207.
11. Guarino, R.D., Perez, D.M., and Piascik, M.T. 1996. Recent advances in the molecular pharmacology of the α_1-adrenergic receptors. *Cell Signal.* **8**:323–333.
12. Michelotti, G.A., Price, D.T., and Schwinn, D.A. 2000. α_1-adrenergic receptor regulation: basic science and clinical implications. *Pharmacol. Ther.* **88**:281–309.
13. Piascik, M.T., and Perez, D.M. 2001. α_1-Adrenergic receptors: new insights and directions. *J. Pharmacol. Exp. Ther.* **298**:403–410.
14. Rohrer, D.K., and Kobilka, B.K. 1998. G protein-coupled receptors: functional and mechanistic insights through altered gene expression. *Physiol. Rev.* **78**:35–52.
15. Koch, W.J., Lefkowitz, R.J., and Rockman, H.A. 2000. Functional consequences of altering myocardial adrenergic receptor signaling. *Annu. Rev. Physiol.* **62**:237–260.
16. Cavalli, A., et al. 1997. Decreased blood pressure response in mice deficient of the α_{1b}-adrenergic receptor. *Proc. Natl. Acad. Sci. USA.* **94**:11589–11594.
17. Deng, X.F., Chemtob, S., and Varma, D.R. 1996. Characterization of α_{1D}-

adrenoceptor subtype in rat myocardium, aorta and other tissues. *Br. J. Pharmacol.* **119**:269–276.
18. Zuscik, M.J., et al. 2001. Hypotension, autonomic failure, and cardiac hypertrophy in transgenic mice overexpressing the α_{1B}-adrenergic receptor. *J. Biol. Chem.* **276**:13738–13743.
19. Arai, K., et al. 1999. Characterization of the mouse α_{1d}-adrenergic receptor gene. *Jpn. J. Pharmacol.* **81**:271–278.
20. Kaestner, K.H., Silberg, D.G., Traber, P.G., and Schutz, G. 1997. The mesenchymal winged helix transcription factor Fkh6 is required for the control of gastrointestinal proliferation and differentiation. *Genes Dev.* **11**:1583–1595.
21. Yagi, T., et al. 1993. A novel negative selection for homologous recombinants using diphtheria toxin A fragment gene. *Anal. Biochem.* **214**:77–86.
22. Schlager, G. 1966. Systolic blood pressure in eight inbred strains of mice. *Nature*. **212**:519–520.
23. Tanoue, A., Endo, F., Kitano, A., and Matsuda, I. 1990. A single nucleotide change in the prolidase gene in fibroblasts from two patients with polypeptide positive prolidase deficiency. Expression of the mutant enzyme in NIH 3T3 cells. *J. Clin. Invest.* **86**:351–355.
24. Sabath, D.E., Broome, H.E., and Prystowsky, M.B. 1990. Glyceraldehyde-3-phosphate dehydrogenase mRNA is a major interleukin 2-induced transcript in a cloned T-helper lymphocyte. *Gene.* **91**:185–191.
25. Alonso-Llamazares, A., et al. 1995. Molecular cloning of α_{1d}-adrenergic receptor and tissue distribution of three alpha 1-adrenergic receptor subtypes in mouse. *J. Neurochem.* **65**:2387–2392.
26. Shibata, K., et al. 1995. KMD-3213, a novel, potent, α_{1a}-adrenoceptor-selective antagonist: characterization using recombinant human α_1-adrenoceptors and native tissues. *Mol. Pharmacol.* **48**:250–258.
27. Krege, J., Hodgin, J., Hagaman, J., and Smithies, O. 1995. A computerized system for measuring blood pressure in mice. *Hypertension*. **25**:1111–1115.
28. Chruscinski, A.J., et al. 1999. Targeted disruption of the β2 adrenergic receptor gene. *J. Biol. Chem*. **274**:16694–16700.
29. Tanaka, N., et al. 1996. Transthoracic echocardiography in models of cardiac disease in the mouse. *Circulation.* **94**:1109–1117.
30. Nasa, Y., et al. 1998. Effects of the antihypertensive agent, cicletanine, on noradrenaline release and vasoconstriction in perfused mesenteric artery of SHR. *Br. J. Pharmacol*. **123**:427–434.
31. Munson, P.J., and Rodbard, D. 1980. Ligand: a versatile computerized approach for characterization of ligand-binding systems. *Anal. Biochem.* **107**:220–239.
32. Jacobs, M.C., Lenders, J.W., Willemsen, J.J., and Thien, T. 1995. Chronic α1-adrenergic blockade increases sympathoneural but not adrenomedullary activity in patients with essential hypertension. *J. Hypertens*. **13**:1837–1841.
33. Kenny, B.A., Chalmers, D.H., Philpott, P.C., and Naylor, A.M. 1995. Characterization of an α_{1D}-adrenoceptor mediating the contractile response of rat aorta to noradrenaline. *Br. J. Pharmacol.* **115**:981–986.
34. Piascik, M.T., et al. 1995. The specific contribution of the novel α_{1D} adrenoceptor to the contraction of vascular smooth muscle. *J. Pharmacol. Exp. Ther.* **275**:1583–1589.
35. Buckner, S.A., Oheim, K.W., Morse, P.A., Knepper, S.M., and Hancock, A.A. 1996. α_1-adrenoceptor-induced contractility in rat aorta is mediated by the α_{1D}-subtype. *Eur. J. Pharmacol.* **297**:241–248.
36. Gisbert, R., Noguera, M.A., Ivorra, M.D., and D'Ocon, P. 2000. Functional evidence of a constitutively active population of α_{1D}-adrenoceptors in rat aorta. *J. Pharmacol. Exp. Ther*. **295**:810–817.
37. Piascik, M.T., et al. 1997. Immunocytochemical localization of the α_{1B} adrenergic receptor and the contribution of this and the other subtypes to vascular smooth muscle contraction: analysis with selective ligands and antisense oligonucleotides. *J. Pharmacol. Exp. Ther.* **283**:854–868.
38. Hrometz, S.L., et al. 1999. Expression of multiple α_1-adrenoceptors on vascular smooth muscle: correlation with the regulation of contraction. *J. Pharmacol. Exp. Ther.* **290**:452–463.
39. Rudner, X.L., et al. 1999. Subtype specific regulation of human vascular α_1-adrenergic receptors by vessel bed and age. *Circulation.* **100**:2336–2343.
40. Guimaraes, S., and Moura, D. 2001. Vascular adrenoceptors: an update. *Pharmacol. Rev.* **53**:319–356.
41. Milano, C.A., et al. 1994. Myocardial expression of a constitutively active α_{1B}-adrenergic receptor in transgenic mice induces cardiac hypertrophy. *Proc. Natl. Acad. Sci. USA.* **91**:10109–10113.
42. Akhter, S.A., et al. 1997. Transgenic mice with cardiac overexpression of α_{1B}-adrenergic receptors. In vivo α_1-adrenergic receptor-mediated regulation of β-adrenergic signaling. *J. Biol. Chem.* **272**:21253–21259.
43. O'Connell, T.D., et al. 2000. α_1-Adrenergic receptors are required for normal postnatal growth of the heart. *Circulation.* **102**:II-197. (Abstr.)
44. Rudner, X.L., et al. 1999. Subtype specific regulation of human vascular α_1-adrenergic receptors by vessel bed and age. *Circulation.* **100**:2336–2343.
45. Villalobos-Molina, R., and Ibarra, M. 1996. α_1-Adrenoceptors mediating contraction in arteries of normotensive and spontaneously hypertensive rats are of the α_{1D} or α_{1A} subtypes. *Eur. J. Pharmacol.* **298**:257–263.
46. Villalobos-Molina, R., Lopez-Guerrero, J.J., and Ibarra, M. 1999. Functional evidence of α_{1D}-adrenoceptors in the vasculature of young and adult spontaneously hypertensive rats. *Br. J. Pharmacol.* **126**:1534–1536.
47. Ibarra, M., Pardo, J.P., Lopez-Guerrero, J.J., and Villalobos-Molina, R. 2000. Differential response to chloroethylclonidine in blood vessels of normotensive and spontaneously hypertensive rats: role of α_{1D}- and α_{1A}-adrenoceptors in contraction. *Br. J. Pharmacol.* **129**:653–660.
48. Ibarra, M., Terron, J.A., Lopez-Guerrero, J.J., and Villalobos-Molina, R. 1997. Evidence for an age-dependent functional expression of α_{1D}-adrenoceptors in the rat vasculature. *Eur. J. Pharmacol.* **322**:221–224.
49. Chen, L., Xin, X., Eckhart, A.D., Yang, N., and Faber, J.E. 1995. Regulation of vascular smooth muscle growth by α_1-adrenoreceptor subtypes in vitro and in situ. *J. Biol. Chem.* **270**:30980–30988.
50. Xin, X., Yang, N., and Faber, J.E. 1999. Platelet-derived growth factor inhibits α_{1D}-adrenergic receptor expression in vascular smooth muscle cells in vitro and ex vivo. *Mol. Pharmacol.* **56**:1143–1151.